Anti-windup Control of Active Magnetic Bearings Subject to Voltage Saturation

Jinxiang Zhou[a], Jiancheng Fang[a], Yin Zhang[a], Yinxiao Jiang[a]

[a] BeiHang University, XueYuan Road No.37, HaiDian District, Beijing, China, zhoujinxiang99@gmail.com

***Abstract*—Active magnetic bearings (AMBs) have been widely applied in industrial rotating machinery. Power amplifier as an essential actuator of the AMB faces the limitation of DC bus voltage. A simple approach is to increase the voltage to a high value, but it has to deal with large current ripples and a low resolution. Other than the ordinary method, this paper addresses to the anti-windup control of AMB that aims to eliminate the adverse effect of the voltage saturation. The anti-windup algorithm is an addition to the nominal linear controller. And only when the saturation occurs is it activated. The stability is guaranteed by the procedure of calculating the linear matrix inequality (LMI) form of the regional Lyapunov stability. Simulation test is done to verify the proposed controller. Finally in the motor drive experiment, the axial AMB equipped in the prototype supports the thrust force. With the load changes, the performance of the anti-windup controller is demonstrated.**

***Keywords*—AMB, voltage saturation, anti-windup control**

I. INTRODUCTION

Active magnetic bearings (AMBs) have so many advantages such as non-contact, no friction, no wear, long life, low noise, small vibration, no lubrication requirement, and adjustable dynamic performance [1, 2]. Due to the character of its natural unstable pole, each AMB needs a control loop. A typical AMB system consists of sensors, signal processers, power amplifiers, electromagnets (EMs) and ferromagnetic rotor components. Power amplifier converts the control signals to the changes of the current in the EM's windings, so that it can provide the magnetic force to suspend the rotor stably.

Nowadays Pulse Width Modulation (PWM) switch technic is quite common adopted in power converters, since it is simple, convenient, and efficient. This kind of power electronics together with EM's coils can be classified into the Class-D amplifier, which is generally modeled as a controlled voltage source [3]. As to the classification of the AMB control mode, there are current control mode, voltage control mode, and flux control mode reviewed in [1, 4]. No matter in which mode, the physical realization is the same way that the voltage across the coil is changed. So the DC bus voltage is the inherent restriction of the AMB PWM amplifier. And the voltage saturation was once discussed in the Annex C of the standard ISO 14839-2:2004.

In most controller design procedures, based on the small signal linear model, we can get a preliminary result. Then through the regulation to enhance the robustness, and maybe making some compromise, the effect of the voltage saturation is not significant. However, when the AMB is applied in some special industrial cases, or even in the rotor levitating moments, the windup phenomenon caused by the voltage saturation is observed, and may lead to a failure. Some AMB equipped in power motor products designed by famous manufactures such as Danfoss Turbocor, SKF and Synchrony, have employed a high power DC voltage of 250V or higher.

Since the high voltage across the switch converters causes more current ripples, which are the noise to the current sensors. And to the same PWM carrier frequency, the resolution of the amplifiers is reduced as the range of the output is widened. Besides, a low voltage is adequate for the most time of the AMB regular operation. So there are some works that have been done to seek solutions in other ways. For the low- and zero-bias AMB, a nonlinear controller based on Teel's small gain saturation theory, was reported in [5] to solve the voltage saturation. Lee, R. M. [6] and Haiping, Du [7] proposed fuzzy control methods subject to their special disturbance models, that is to solve the saturation problem in the AMB of milling machine.

This paper is to apply the anti-windup (AW) control synthesis to the AMB controller design in the 100KW 32000r/min magnetic levitation motor. The AMB power bus voltage 90V is selected. In the motor drive experiment, two rotors are attached to each other by a rope coupling. There is an additional thrust force upon the axial AMBs when the motor drives the generator. This changing load often causes the voltage saturation of the axial AMB amplifier, leading to a large-scale long-period oscillation.

In both fields of academy and engineering, the anti-windup problem has been studied for a quite long history. Until the last two decades, uniform control structure and the linear matrix inequality (LMI) approach have become the consensus [8]. The general anti-windup control structure is shown as Figure 1.

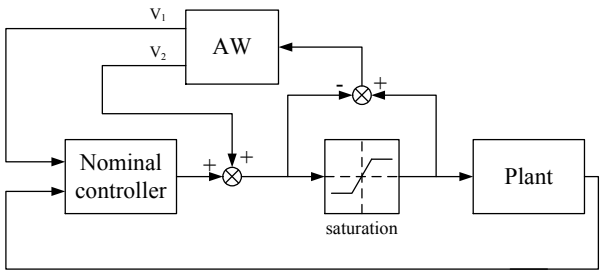

Figure 1. General anti-windup control structure

The AW refers to the anti-windup block, which takes the saturation information as inputs, and outputs two vectors. The design procedure is divided into the following two steps:

- Design the nominal controller without the consideration of the saturation.
- Transform the saturation function to the sector condition, and then use the LMI to search an AW matrix to minimize the optimization goal.

As to the unstable plant, a local case region of stability domain is guaranteed under the constraints of the actuator's output [9]. The anti-windup synthesis proposed by da Silva, J. M. G. etc. [10], takes the maximum stability region as the optimization goal. The methods based on L_2 norm performance are given in [11, 12]. Due to the simple procedure and few parameters, the former static compensator [10] is easier to calculate and to put into engineering practice. And this method is further clarified and promoted in [13]. So based on this theory, we takes the anti-windup algorithm into the axial AMB control. Although this work is done to a one degree of freedom (DOF) AMB, it could be easily applied to the control of radial AMBs if it is wanted.

The next section presents the structure of the axial AMB and derives its mathematical model. To be universal, section 3 gives control system configuration and the nominal controller design, which includes the PID form of the displacement signal and a current feedback loop. Then the anti-windup compensator is constructed and the LMIs are solved to get the AW matrix. Besides the simulation, the experiments using the AMB prototype with load cases are present in the following part. At last, the conclusion is made that the negative influence of the voltage saturation can be improved.

II. STRUCTURE OF THE AXIAL AMB

The axial magnetic bearing of the prototype employs the structure that is proposed in [14], but differs in dimensions and parameters. Figure 2 shows the profile of the thrust magnetic bearing that is tested in this work. Although it is named permanent-magnet-biased hybrid magnetic bearing in [14], there is little difference in the linear model for control consideration, as we will see in the Eq.(3). So in the opinion of [1], this kind hybrid magnetic bearing is still classified into the AMB.

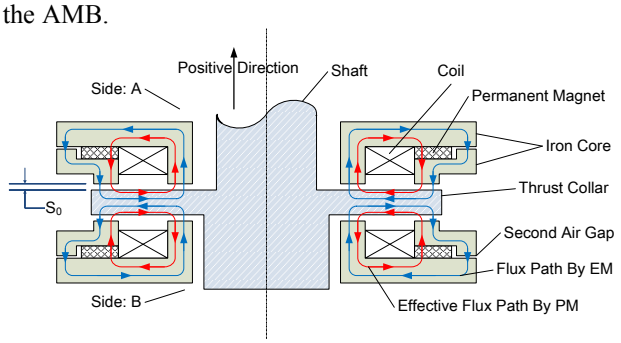

Figure 2. Configuration of axial magnetic bearing

The control flux is generated by the EMs, and flows across the iron cores, thrust collar, air gaps of the poles, and a second air gap. Two axially magnetized ring magnets act as permanent magnets (PMs). The flux circuit of PM has two branches. One flows across the second air gap, the other flows across the pole air gap providing the bias flux.

The cross sections in each pole air gap of the inner ring and the outer have the equal area A (m^2). The coils of the upper EM and the below are connected in series. Assuming the shaft has a positive displacement x (m) to the nominal position S_0 (m) and there is a current i (A) in the coil, the total magnetic force $F(x,i)$ (N) upon the collar can be calculated as follows:

$$F(x,i)=\frac{\phi_a^{\,2}}{2\mu_0 A}+\frac{\phi_a^{\,2}}{2\mu_0 A}-\frac{\phi_b^{\,2}}{2\mu_0 A}-\frac{\phi_b^{\,2}}{2\mu_0 A} \tag{1}$$

$$\begin{cases}\phi_a=\phi_{pa}+\phi_{ca}=\dfrac{F_{pm}\mu_0 A}{2(S_0-x)}+\dfrac{Ni\mu_0 A}{2(S_0-x)+S_2A/A_2}\\ \phi_b=\phi_{pb}-\phi_{cb}=\dfrac{F_{pm}\mu_0 A}{2(S_0+x)}-\dfrac{Ni\mu_0 A}{2(S_0+x)+S_2A/A_2}\end{cases} \tag{2}$$

where ϕ denotes the magnetic flux, and the subscript a, b, p, c refers to the side a, b, the bias flux by the permanent magnet, the control flux, respectively. μ_0 denotes the permeability of air. F_{pm} is the magnetomotive force (MMF) of the PM. S_2 and A_2 denote the width and cross section area of the second air gap.

The function of $F(x,i)$ can be expanded in Taylor's series at the equilibrium point. It can be predicted that the high order terms contain the same order of μ_0, which are quite small values. So a familiar linear term can be expressed in Eq.(3):

$$F(x,i)=K_x\cdot x+K_i\cdot i \tag{3}$$

where

$$\begin{cases}K_x=\left.\dfrac{\partial f}{\partial x}\right|_{\substack{x=0\\i=0}}=\dfrac{\mu_0 F_{pm}^2 A}{S_0^3}\\ K_i=\left.\dfrac{\partial f}{\partial i}\right|_{\substack{x=0\\i=0}}=\dfrac{2\mu_0 N F_{pm} A}{S_0(2S_0+S_2A/A_2)}\end{cases} \tag{4}$$

K_x and K_i denote the displacement stiffness and current stiffness.

III. SYSTEM MODEL AND THE NOMINAL CONTROLLER

Figure 11 is the general schematic diagram of the AMB control system. A chip of DSP is used to realize the control algorithm. The PWM drive signals are produced in the FPGA. The amplifier circuits apply the H bridge topology, which consists of four power MOSFETs. The control signal is modulated in the varying voltage across the EM coil.

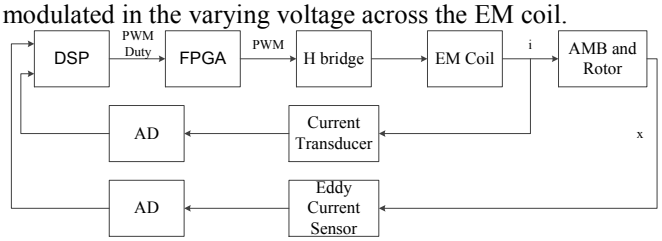

Figure 3. Control loop of the AMB

As the coils of two sides connected in series, the voltage can be calculated by the Eq.(5).

$$u=(R_a+R_b)\cdot i+N\frac{d\phi_a}{dt}+N\frac{d\phi_b}{dt} \tag{5}$$

Applying (2) to (5), and combining like terms, a simplified equation is obtained.

$$u = (R_a + R_b)\cdot i + \frac{2N^2\mu_0 A}{2S_0 + S_2 A / A_2}\cdot\frac{di}{dt} \triangleq R\cdot i + L\cdot\frac{di}{dt} \tag{6}$$

As to one DOF, the state vector X is defined as follows:

$$X = \begin{bmatrix} x & \dot{x} & i \end{bmatrix}^T \tag{7}$$

The system model in state space form can be easily obtained.

$$\begin{aligned} \dot{X}(t) &= A\cdot X(t) + B\cdot u(t) \\ Y(t) &= C\cdot X(t) \end{aligned} \tag{8}$$

The matrices, A, B, C are given as:

$$\begin{aligned} A &= \begin{bmatrix} 0 & 1 & 0 \\ K_s/m & 0 & K_i/m \\ 0 & 0 & -R/L \end{bmatrix} \\ B &= \begin{bmatrix} 0 & 0 & V_c \end{bmatrix}^T \\ C &= -diag\begin{pmatrix} S_x & S_x & S_i \end{pmatrix} \end{aligned} \tag{9}$$

where V_c denotes the DC bus voltage, and S_x, S_i represent the position sensor's and current transducer's proportional factors, including the scale factor of AD chips.

It should be noticed about the meaning of the controller output u_c. In the actual system, it is realized by the PWM duty δ, which is bounded in the section of 0 to 1. Because of the H bridge topology, the full positive DC bus voltage is upon the coil when δ is 1, and the full negative voltage is when δ is 0. And a proper scale transform is needed. And in the abstract model, the plant input u and the controller output u_c have the relationship as:

$$u = sat(u_c) = \begin{cases} 1 & u_c > 1 \\ u_c & -1 \le u_c \le 1 \\ -1 & u_c < -1 \end{cases} \tag{10}$$

Although numerous modern control strategies applied in the AMB have been reported in academics, the PID control is still the primary choice of the industry. The reason that we take the PID as the original controller is its concise form and universality. So the parts of the anti-windup study will be prominent.

Specifically, the PID progress of the position signal contains a first-order derivative filter. A proportional feedback of the current signal is added to the operation result. The state form of the nominal controller is expressed as:

$$\begin{aligned} \begin{bmatrix} \dot{\eta}_1 \\ \dot{\eta}_2 \end{bmatrix} &= \begin{bmatrix} 0 & 0 \\ 0 & -1/T_f \end{bmatrix}\bullet\begin{bmatrix} \eta_1 \\ \eta_2 \end{bmatrix} + \begin{bmatrix} I & 0 & 0 \\ 0 & D/T_f & 0 \end{bmatrix}\bullet Y \\ u_c &= K_{amp}\bullet\begin{bmatrix} 1 & 1 \end{bmatrix}\bullet\begin{bmatrix} \eta_1 \\ \eta_2 \end{bmatrix} + K_{amp}\bullet\begin{bmatrix} P & 0 & I_{co} \end{bmatrix}\bullet Y \end{aligned} \tag{11}$$

where I_{co} denotes the coefficient of current feedback, K_{amp} denotes the factor that regulars the output's scale, P, I, D, and T_f denote the coefficients of the proportion, integration, differentiation, and derivative filter respectively.

Without consideration of the constraint (10), the stability and performance of the control system are checked by the Nyquist diagram (Figure 4) and magnitude plot of sensitivity function (Figure 5). Obviously, the AMB system is well stabilized. And the peak magnitude of the sensitivity function is 1.8, satisfying the performance requirements of most applications. The specific values of the prototype are given in TABLE I.

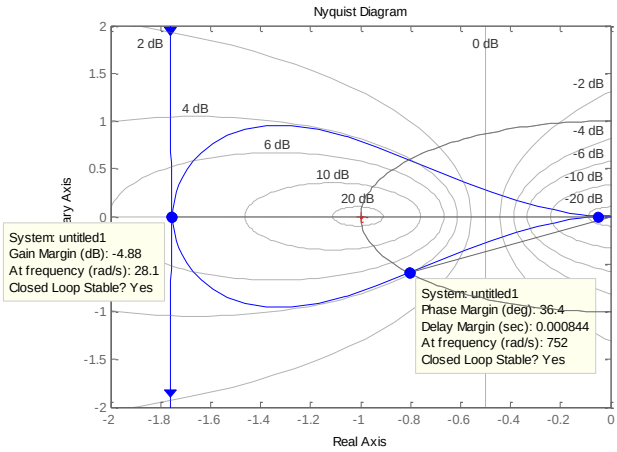

Figure 4. Nyquist diagam of the control system

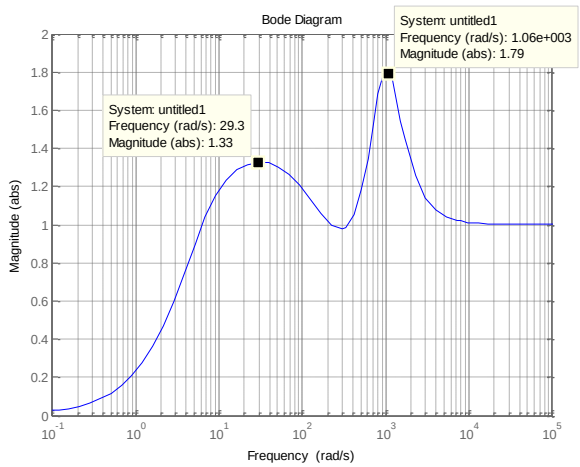

Figure 5. Magnitude plot of sensitivity function

TABLE I. PARAMETER VALUES OF THE AMB SYSTEM

Parameter	Value	Parameter	Value
K_x	3200 N/mm	P	9.6
K_i	960 N/A	I	23.6
L	0.34 H	D	0.038
R	50.8 Ω	T_f	0.038/1000
m	20.6 Kg	I_{co}	8.6
V_c	90 V	K_{amp}	0.64/1000

IV. ANTI-WINDUP COMPENSATOR DESIGN

In the last section, it has been mentioned that the controller output is restricted in Eq.(10). This is a typical saturation of the actuator output. When the control signal reaches or overflows the boundary, there is ineluctable performance degradation of the control system. The missing information ($sat(u_c) - u_c$) can be easily picked up in the digital processor. So an anti-windup term $E_c(sat(u_c) - u_c)$ is added to the controller to mitigate the undesirable influence of windup. Here E_c is a constant matrix of appropriate order, so this is called the static anti-windup compensator [12].

Considering the anti-windup strategy, rewrite the dynamic controller (11) and the closed-loop system (8), we gets:

$$\begin{aligned}
\dot{X}(t) &= AX(t) + Bsat(u_c(t)) \\
Y(t) &= CX(t) \\
\dot{X}_c(t) &= A_c X_c(t) + B_c Y(t) + \begin{bmatrix} I_2 & 0 \end{bmatrix} E_c \varphi(u_c) \\
u_c(t) &= C_c X_c(t) + D_c Y(t) + \begin{bmatrix} 0 & I_1 \end{bmatrix} E_c \varphi(u_c) \\
\varphi(u_c) &= sat(u_c(t)) - u_c(t)
\end{aligned} \tag{12}$$

where X_c denotes the state vector of the controller (11), A_c, B_c, C_c, D_c are abbreviations of the matrixes in (11).

The benefit of the (12) is obvious that when there is no saturation the system is the original one with no difference, when saturation occurs the controller's input and output get modified.

Now define an extended state vector:

$$\xi = \begin{bmatrix} X & X_c \end{bmatrix}^T = \begin{bmatrix} x & \dot{x} & i & \eta_1 & \eta_2 \end{bmatrix}^T \tag{13}$$

then the closed-loop system reads:

$$\begin{aligned}
\dot{\xi} &= \alpha\xi + (\beta + \gamma_1 E_c)\varphi(u_c) \\
u_c &= \lambda\xi + \gamma_2 E_c \varphi(u_c)
\end{aligned} \tag{14}$$

where

$$\begin{aligned}
\alpha &= \begin{bmatrix} A + BD_cC & BC_c \\ B_cC & A_c \end{bmatrix}, \beta = \begin{bmatrix} B \\ 0 \end{bmatrix} \\
\gamma_1 &= \begin{bmatrix} B\begin{bmatrix} 0 & I_1 \end{bmatrix} \\ I_2 & 0 \end{bmatrix}, \gamma_2 = \begin{bmatrix} 0 & I_1 \end{bmatrix} \\
\lambda &= \begin{bmatrix} D_cC & C_c \end{bmatrix}
\end{aligned} \tag{15}$$

The Theorem 1 in [13] gives the sufficient condition to calculate the asymptotic stability region for this problem. The proofs to it could be explored in the similar procedures of [10]. Here we rewrite the theorem in the form special to system (14) as follows:

Theorem 1: If there exist a symmetric positive definite matrix $W \in \mathbb{R}^{5\times5}$, a vector $Y \in \mathbb{R}^{1\times5}$, a vector $Z \in \mathbb{R}^{3\times1}$, and a positive scalar *S* satisfying

$$\begin{bmatrix} W\alpha^T + \alpha W & \beta S + \gamma_1 Z - W\lambda^T - Y^T \\ * & -2S - \gamma_2 Z - Z^T\gamma_2^T \end{bmatrix} < 0 \tag{16}$$

$$\begin{bmatrix} W & Y^T \\ * & 1 \end{bmatrix} \geq 0 \tag{17}$$

then the gain matrix $E_c = Z \cdot S^{-1}$ is such that the ellipsoid $\varepsilon(W) = \left\{ \xi \in \mathbb{R}^{5\times1} \middle| \xi^T W^{-1} \xi \leq 1 \right\}$ is an asymptotic stability region for system (14).

The LMI (16) is obtained from the Lyapunov candidate function:

$$V(\xi) = \xi^T(t) \cdot P \cdot \xi(t),\ P = P^T = W^{-1} > 0,\ and\ \dot{V}(\xi) < 0 \tag{18}$$

A sector condition $\varphi^T(u_c) \cdot S^{-1} \cdot (sat(u_c) + \omega) \leq 0$ where ω satisfying $|\omega| \leq 1$ is applied in (18). And LMI (17) implies ω is constructed from the set $\varepsilon(W)$ and *Y*.

Based on the theorem 1, the direct objective to search the matrix E_c is to maximize the volume of $\varepsilon(W)$, which could be quantified by the determinant of the matrix W^{-1}. So the solution to the anti-windup design is transformed to an optimization problem in the LMI form. The optimization goal should be set as

minimize: $J = -log(det(W^{-1})) = log(det(W))$

Unfortunately, we could not access a proper solver to this nonlinear goal. To be simplified, the $\varepsilon(W)$ is searched to maximize the size along two directions of the controller states. A linear objective is obtained by:

$$\begin{aligned}
&(\varepsilon v_1)^T \cdot W^{-1} \cdot (\varepsilon v_1) \leq 1 \\
&(\varepsilon v_2)^T \cdot W^{-1} \cdot (\varepsilon v_2) \leq 1 \\
&v_1 = \begin{bmatrix} 0 & 0 & 0 & 1 & 0 \end{bmatrix}^T \\
&v_1 = \begin{bmatrix} 0 & 0 & 0 & 0 & 1 \end{bmatrix}^T \\
&\max \varepsilon \triangleq \frac{1}{\sqrt{\mu}}
\end{aligned} \tag{19}$$

The inequalities (19) could be further written in matrix form (20). Besides, from the forth equation in (12), it can be found that $E_c = \begin{bmatrix} * & * & -1 \end{bmatrix}$ is an undesirable singular point, making the controller output u_c meaningless. So constraint (21) is added to avoid converging to that point. The final optimization problem reads as follows:

minimize: μ

subject to: $W > 0, S > 0$

LMIs (16), *and* (17)

$$\begin{bmatrix} \mu & v_1^T \\ v_1 & W \end{bmatrix} \geq 0, \begin{bmatrix} \mu & v_2^T \\ v_2 & W \end{bmatrix} \geq 0 \tag{20}$$

$$\left| \begin{bmatrix} 0 & 0 & 1 \end{bmatrix} \cdot Z + S \right| > 0.1 \cdot S \tag{21}$$

The toolbox YALMIP in MATLAB is used in the numerical calculation. To avoid large conditions of matrixes during the computation, the state vector (13) is normalized by:

$$\bar{\xi} = T \cdot \xi = \begin{bmatrix} \xi_i / \max(\xi_i) \end{bmatrix}^T \tag{22}$$

where $\max(\xi_i)$ denotes the max value or estimated max value of the respective element. The matrixes in (15) are transformed by *T* and T^{-1} accordingly. The detailed process is simple and omitted here.

Adopting the data listed in TABLE I, the results of the optimization is given as:

$\mu = 0.348$, $E_c = \begin{bmatrix} 37.5 & -263.3 & -0.6 \end{bmatrix}^T$.

Since the E_c is obtained, there is a reverse procedure to put it back to the actual control system. All scale factors should be paid special attentions to. Otherwise it may lead to mistakes according to our experience. The next section will demonstrate the simulation and experiments results.

V. SIMULATION AND EXPERIMENT

The first occasion that the windup phenomenon in AMB caused our interest is the levitating moments of the prototype rotor. The controller parameters first designed by the system model without consideration of the saturation have a poor performance in the actual system.

The auxiliary thrust bearing restricts the position of the rotor to -0.5mm to 0.5mm. When the AMB control board is powered on, the first results of controller must reach the

limits. On the other hand, the amplifier circuit is powered on after the drive signals are working properly. During this delay time of 0.1 seconds, the integration register of the controller may be overflowing. All these conditions result in a long time of the output saturation. The simulation of the AMB under this condition is shown in Figure 6. The Figure 7 is the plot of the calculated voltage values according to PWM duty during this time. Although the PWM duty in actual system cannot be exact 0 or 1 because of the security setting of dead-times. It could be still seen that the voltage has reached the limitation of DC bus in the starting time. And correspondingly there is a large overstrike in the displacement of the shaft. The black dash line simulates the condition that the voltage is unlimited. After applying the anti-windup strategy, the times of overstrike and settle are reduced.

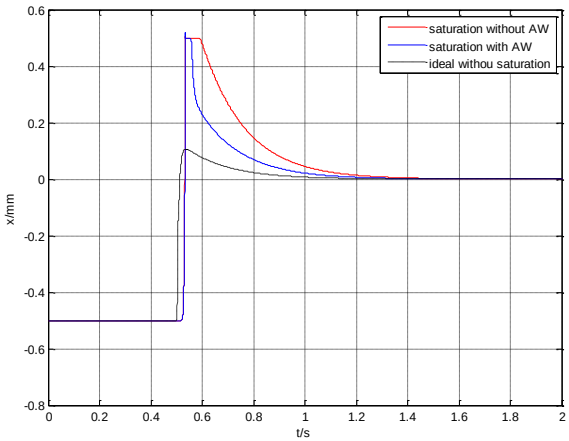

Figure 6. The simulation plot of rotor position during levitating

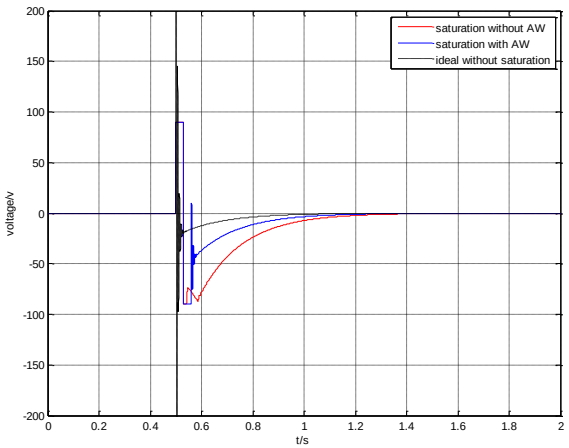

Figure 7. The computed voltage values during levitating

Figure 8 and Figure 9 simulate the occasions the thrust magnetic bearing carrying loads. The shaft is working at the rotation speed of 12000rpm. So a 200Hz displace sinusoid disturbance is added to the simulation. At the time of 0.5s, a first step 300N axial force is upon the shaft. Without controller saturation occurs, there is no difference in the three. At the time of 2.5s, another step 500N axial force is added. The total force is up to 800N and the output voltage reaches to the limits 90V. In the ideal conditions, the magnetic bearing still works well except for a little large oscillation. But when the voltage saturation is considered, the magnetic bearing could not hold the rotor properly. The shaft touches down on the auxiliary bearing and causes serious collisions. As to the robustness of the controller, the system recovered after about 0.25s without AW control. As to the controller with AW, the touchdown behavior is still not avoided, but the system recovers faster.

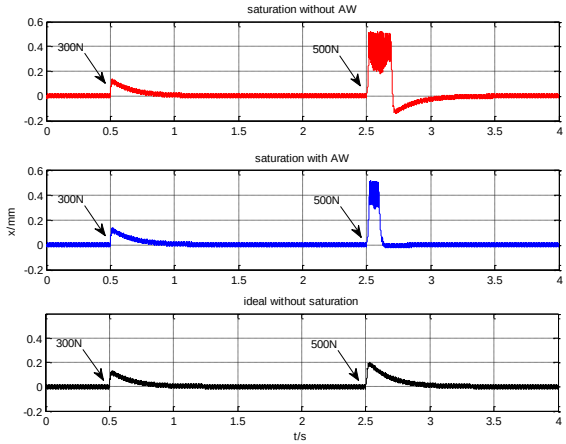

Figure 8. The simulation plot of rotor position when carrying loads

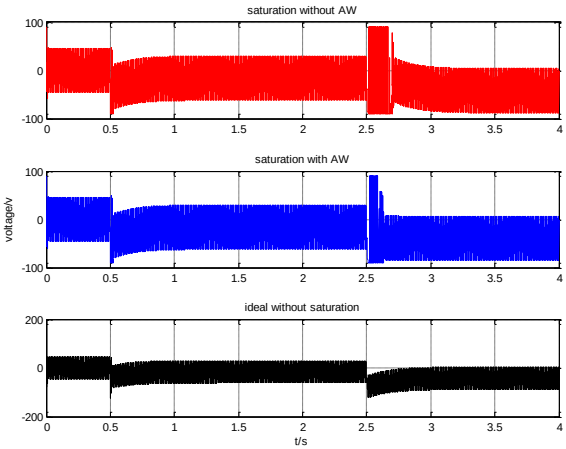

Figure 9. The computed voltage values when carrying loads

In the experiments of real AMB system, the comparison results of the AW control are given in Figure 10. The data are taken from the signals of the displacement sensor. It outputs voltage signals of 0.25V to 2.75V, corresponding to the shaft displacement -0.5mm to 0.5mm. It could be seen that the controller with anti-windup strategy have the advantage of a fast recovery speed when the saturation occurs.

Figure 11 gives the photo of the site of the motor drive experiment. In the picture, two prototypes are both equipped with AMBs. Two shafts are connected by a rope coupling. The generator armature is connected with resistances to produce resisting moment. When the fiber ropes conducts the motor's torque, an axial tensile force is generated simultaneously. The torque is determined by the rotation speed and the resistance's value. So when we switch the resistance's value to test the motor power, the axial force is changed suddenly. This axial impulse upon the magnetic bearing may lead to the voltage saturation, and caused a long

time recovery. Due to the flexible connection of the rope coupling, it is hard to model and quantify the change of the axial force. So the controller must be strong robust. Figure 12 is on the circumstance that the rotor is operating at the speed of 12000rpm, and the generator's resistance is switched on to 1.2Ω from the off state. Although there is no significant difference between the two plots, the anti-windup effect still could be found in the period of the oscillations.

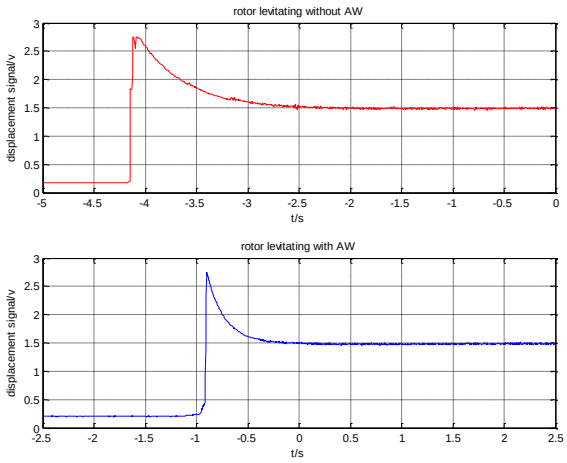

Figure 10. The signal of the real shaft displacement during levitating

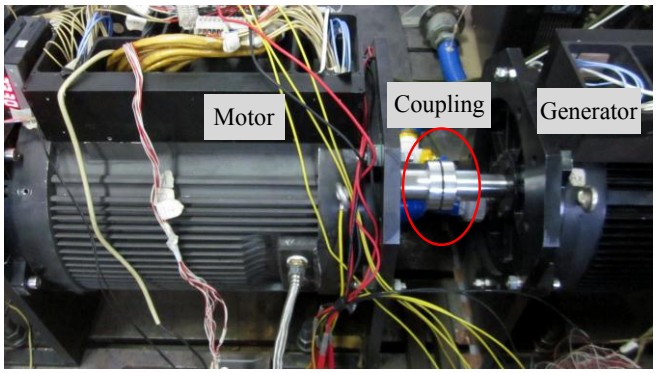

Figure 11. Site of motor drive experiment

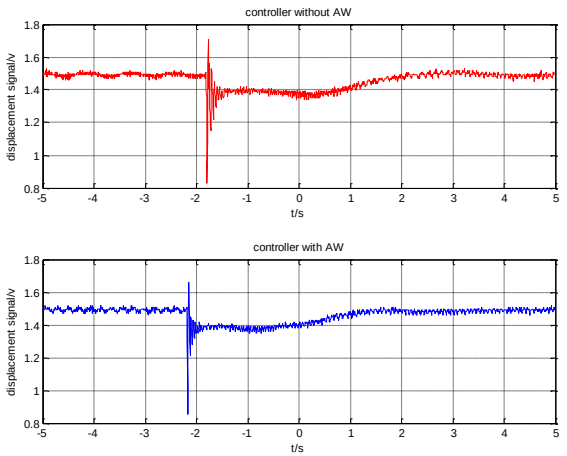

Figure 12. The displacement of the rotor with axial load changes

VI. CONCLUSION

Since the anti-windup control has been a hot topic in control theorem, and this paper aims to examine the application in the AMB control. An actual axial AMB is taken into the anti-windup controller design. One advantage of the strategy is that there is no change of the nominal controller when the voltage saturation does not occur. The other is that it improves the recovery performance of the system when there is saturation. Through the simulation and prototype experiments, the anti-windup control is proven to be a choice to mitigate the negative influence of the AMB voltage saturation.

REFERENCES

[1] Schweitzer, G. and E.H. Maslen, *Magnetic bearings: theory, design and application to rotating machinery* 2009.

[2] Schweitzer, G., *Applications and Research Topics for Active Magnetic Bearings*. Iutam Symposium on Emerging Trends in Rotor Dynamics, ed. K. Gupta. Vol. 25. 2011, New York: Springer. 263-273.

[3] Deslauriers, I., N. Avdiu, and B.T. Ooi, *Naturally sampled triangle carrier PWM bandwidth limit and output spectrum.* Ieee Transactions on Power Electronics, 2005. **20**(1): p. 100-106.

[4] Tsiotras, P. and B.C. Wilson, *Zero-and low-bias control designs for active magnetic bearings.* Control Systems Technology, IEEE Transactions on, 2003. **11**(6): p. 889-904.

[5] Tsiotras, P. and M. Arcak, *Low-bias control of AMB subject to voltage saturation: State-feedback and observer designs.* Control Systems Technology, IEEE Transactions on, 2005. **13**(2): p. 262-273.

[6] Lee, R.M. and N.C. Tsai, *Fuzzy compensator design against windup of a magnetic actuator during milling operation.* Proceedings of the Institution of Mechanical Engineers Part B-Journal of Engineering Manufacture, 2012. **226**(B9): p. 1454-1464.

[7] Haiping, D., et al., *Robust Fuzzy Control of an Active Magnetic Bearing Subject to Voltage Saturation.* Control Systems Technology, IEEE Transactions on, 2010. **18**(1): p. 164-169.

[8] Zaccarian, L. and A.R. Teel, *A common framework for anti-windup, bumpless transfer and reliable designs.* Automatica, 2002. **38**(10): p. 1735-1744.

[9] Teel, A.R., *Anti‐windup for exponentially unstable linear systems.* International Journal of Robust and Nonlinear Control, 1999. **9**(10): p. 701-716.

[10] da Silva, J.M.G. and S. Tarbouriech, *Antiwindup design with guaranteed regions of stability: An LMI-based approach.* Ieee Transactions on Automatic Control, 2005. **50**(1): p. 106-111.

[11] Hu, T., A.R. Teel, and L. Zaccarian, *Anti-windup synthesis for linear control systems with input saturation: Achieving regional, nonlinear performance.* Automatica, 2008. **44**(2): p. 512-519.

[12] Hu, T., A.R. Teel, and L. Zaccarian, *Stability and performance for saturated systems via quadratic and nonquadratic Lyapunov functions.* Ieee Transactions on Automatic Control, 2006. **51**(11): p. 1770-1786.

[13] Tarbouriech, S. and M. Turner, *Anti-windup design: an overview of some recent advances and open problems.* Iet Control Theory and Applications, 2009. **3**(1): p. 1-19.

[14] Fang, J., et al., *A New Structure for Permanent-Magnet-Biased Axial Hybrid Magnetic Bearings.* Magnetics, IEEE Transactions on, 2009. **45**(12): p. 5319-5325.